Chinese Chemical Letters 34 (2023) 107572

Contents lists available at ScienceDirect

Chinese Chemical Letters

journal homepage: www.elsevier.com/locate/cclet

Plasmonic rhenium trioxide self-assembled microtubes for highly sensitive, stable and reproducible surface-enhanced Raman spectroscopy detection

Jingbin Li[a,b,c], Zhiwei Jiao[a,c,*], Junfang Li[b], Hua Bai[b], Guangcheng Xi[b,*]

[a] College of Sciences, China Jiliang University, Hangzhou 310018, China
[b] Institute of Industrial and Consumer Product Safety, Chinese Academy of Inspection and Quarantine, Beijing 100176, China
[c] Key Laboratory of Intelligent Manufacturing Quality Big Data Tracing and Analysis of Zhejiang Province, China Jiliang University, Hangzhou 310018, China

ARTICLE INFO

Article history:
Received 16 March 2022
Revised 16 May 2022
Accepted 26 May 2022
Available online 28 May 2022

Keywords:
SERS
ReO_3
Surface plasmon resonance
Microtubes
Self assembly

ABSTRACT

Compared with noble metals, improving the sensitivity of semiconducting surface-enhanced Raman scattering (SERS) substrates is of great significance to their fundamental research and practical application of Raman spectroscopy. Herein, a simple chemical method is developed to synthesize a rhenium trioxide (ReO_3) microtubes assembled with highly crystalline nanoparticles. The ReO_3 microtubes show a strong and well-defined surface plasmon resonance (SPR) behavior in visible region, which is rare for non-noble metals. As a low-cost SERS substrate, the plasmonic ReO_3 microtubes exhibit a Raman enhancement factor of 8.9×10^5 and a lowest detection limit of 1.0×10^{-9} mol/L for phenolic pollutants. Moreover, these ReO_3 microtubule SERS substrates show excellent chemical stability and can resist the corrosion of strong acids and bases.

At present, SERS has been developed into an advanced, non-destructive analytical technology with superior qualitative capabilities, such as the identification of organic macromolecules and biomolecules, as well as quantitative detection of trace amounts of chemicals [1–9]. The lowest detection limit even can reach single-molecule levels with some specialized treatments [10,11]. Researchers agreed that for a material to perform well in SERS, it must has high sensitivity, excellent chemical stability, exceptional detection reproducibility, and minimal preparation costs [12–15]. So far, people have mainly used Au and Ag nanostructures as SERS substrate materials, mainly because these two types of materials have strong localized-SPR effects [16–19]. Although Au substrates have excellent SERS effect and good chemical stability, their use cost is relatively high. Ag substrates are much cheaper, however, their oxidation resistance is a flaw.

In addition to noble-metal SERS substrates, the rise of semiconductor materials has opened up new directions for the selection of materials for SERS substrates, such as WO_{3-x} [20,21], WO_{3-x}/MoO_2 heterogeneous knot [22], MoO_{3-x} nanosheets [23], Cu_2O nanocrystals [24], $MoTe_2$ ultrathin nanosheets [25], and MoS_2 nanoparticles. [26]. Although these semiconductor SERS substrates often have better biocompatibility and lower cost than noble-metal substrates, their chemical stability is often relatively low, which limits their application. For example, $W_{18}O_{49}$ with abundant oxygen vacancies is easy to be oxidized in air and lose SERS activity. For another example, although the Raman enhancement factor (EF) of $MoTe_2$ nanosheets is as high as 1.0×10^9, it is easily corroded in an acidic environment and is not suitable for many chemical tests. Therefore, the development of sensitive, stable, and low-cost SERS substrates is still an urgent problem in the field of analysis and materials research.

ReO_3 is a unique metallic transition metal oxide, which has a surprising conductivity similar to that of metal Cu [27–29]. For ReO_3, Re^{6+} is a d1 system (the outer electron configuration of rhenium is $5d_5 6s_2$), where the strong hybridization between the Re 5d and O 2p atomic orbitals significantly broadens the 5d conduction band, which gives it strong metallic properties [30,31]. Also due to its rather high free electron density, ReO_3 exhibits a strong localized surface plasmon resonance (LSPR) at the nanoscale. This high free electron density makes ReO_3 a possible SERS substrate candidate, but few researches on their SERS properties have been reported. Herein, a simple chemical method is developed to synthesize a self-assembled microtubular ReO_3 with high chemical durability, which shows strong localized-

* Corresponding authors.
E-mail addresses: jzwgj@163.com (Z. Jiao), xiguangcheng@caiq.org.cn (G. Xi).

https://doi.org/10.1016/j.cclet.2022.05.086
1001-8417/

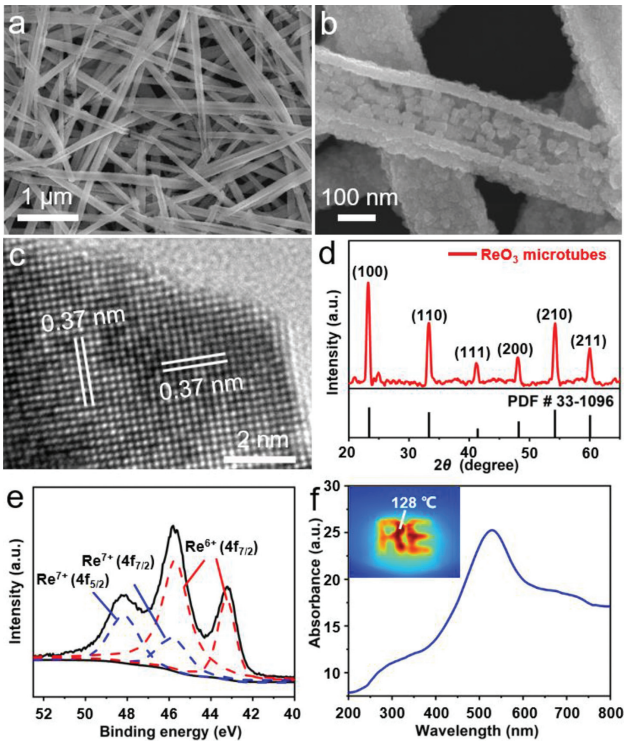

Fig. 1. (a, b) SEM images of ReO_3 microtubes at different magnifications. (c) HRTEM image. (d) X-ray diffraction pattern. (e) The Re 4f spectra of the ReO_3 microtubes. (f) UV–vis-NIR absorption spectrum of ReO_3 microtubes and infrared photothermal image.

SPR behavior and SERS effect. The plasmonic ReO_3 microtubes exhibit a Raman EF of 8.9×10^5 and a lowest detection limit of 1.0×10^{-9} mol/L, which is almost comparable to some noble-metal SERS substrates. Considering that the price of ReO_3 is almost one percent of that of Au, this non-noble metal SERS substrate has great application prospects. The regular microtube structures formed by self-assembly of ReO_3 nanocubes were synthesized by a facile hydrothermal method (Fig. 1a and Fig. S1 in Supporting information). The thickness of these self-assembled microtubes is uniform, the cross-sectional diameter is 200–300 nm, the tube wall thickness is about 40 nm, and the side length of the nanocubic particles is 30–40 nm. Because the tube wall is assembled from much smaller nanocubes (Fig. 1b), the surface of the outer wall is very rough, and many "hot spots" are formed at the junction of each nanocube and nanocube (electromagnetic fields are highly concentrated at the locations). The HRTEM image of the nanocube is shown in Fig. 1c. The clear lattice fringes shown in the figure indicate that the ReO_3 nanocubes have high crystallinity, and the lattice fringes with the interplanar spacing of 0.37 nm can accurately correspond to the (100) crystal plane of the cubic phase ReO_3 nanocrystals. Through powder X-ray diffraction (XRD), we obtained the crystal phase pattern of the ReO_3 microtubes. It can be seen from Fig. 1d that the XRD pattern of the sample can be accurately referred to as cubic phase ReO_3 (JCPDS No: 33–1096). The stronger diffraction peaks also indicate that the product has high crystallinity. The energy dispersive spectrometer (EDS) data shows that the sample only contain Re and O signals (Fig. S2 in Supporting information). The Re/O ratio of the self-assembled microtubes is 1/3.14, which is almost the same as the atomic ratio of ReO_3, which further confirms that the sample is ReO_3. Furthermore, the survey spectrum of X-ray photoelectron spectroscopy (XPS) demonstrated that the sample is highly pure (Fig. S3a in Supporting information). Although the Re 4f spectrum shows a small amount of Re^{7+}, it is still Re^{6+} in the main body (Fig. 1e).

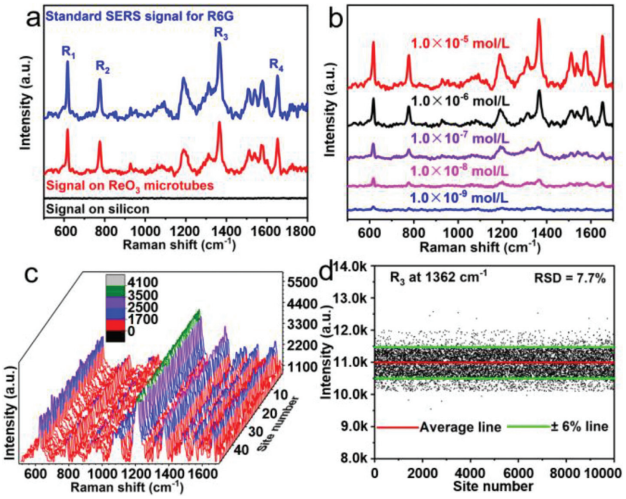

Fig. 2. Confirm the SERS performance, signal uniformity and repeatability of the ReO_3 microtube-substrate. (a) Standard SERS signal for R6G and Raman spectra of 1.0×10^{-5} mol/L R6G on ReO_3 microtubes and bare silicon. (b) SERS spectra of 1.0×10^{-5}-1.0×10^{-9} mol/L R6G on ReO_3 microtubes. (c) SERS spectra of 1.0×10^{-7} mol/L R6G collected from 50 randomly selected locations on ReO_3 microtube substrate. (d) The intensity distribution diagram and RSD value of the characteristic peak of R_3 (1362 cm^{-1}) of 10^4 measuring points.

We evaluated the localized SPR effect of ReO_3 microtubes in the visible light region. Fig. 1f shows the UV–vis-NIR absorption spectrum of ReO_3 microtubes in the air at room temperature. It can be seen that this material exhibits a strong localized SPR effect, and its resonant peak center is located at ~530 nm, which is very close to the commonly used Raman excitation wavelength of 514 nm or 532 nm. It is a favorable condition to generate strong SERS signals that the intrinsic resonance wavelength of the SERS substrate and the Raman excitation wavelength are as close as possible. As shown in Fig. 1f (inset), under the irradiation of a 300 W xenon lamp, the surface temperature of the ReO_3 microtube material rapidly increased from room temperature to 128 °C within 30 s. This excellent photothermal conversion performance further proves the strong localized SPR effect. These results suggest that these ReO_3 microtubules have a very strong SPR effect and are a potential SERS substrate candidate.

As we expected, benefited from the strong localized-SPR effect of the ReO_3 microtubes, their SERS activity is also strong. To evaluate the SERS properties of ReO_3 microtubes, the most commonly used Raman probe molecule rhodamine 6G (R6G) was chosen. Fig. 2a (red spectrum data) shows the SERS spectrum of ReO_3 microtubes of 1.0×10^{-5} mol/L R6G aqueous solution. It can be seen that the ReO_3 microtube SERS-substrate can accurately detect a series of Raman scattering peaks. The four Raman peaks R_1-R_4, which are the most easily identified characteristic peaks of R6G, are located at 612 cm^{-1}, 772 cm^{-1}, 1362 cm^{-1}, and 1651 cm^{-1}, respectively, as well as scattering peaks at other positions, are highly consistent with the Raman spectra of R6G standard (the blue spectrum data in Fig. 2a) . Because these ReO_3 microtubes are in close contact with the silicon wafers, silicon wafers may also contribute to SERS. In order to eliminate this effect, we conducted a controlled experiment. The results show that when a bare silicon wafer is used as the SERS substrate (the black spectrum data in Fig. 2a), the Raman signal of R6G is not obtained, which clearly proves that these enhanced Raman signals are indeed derived from the plasmonic ReO_3 microtubes.

On one hand, the practicality of the SERS substrate is reflected in its detection sensitivity. Fig. 2b shows the Raman spectra of 5 samples of R6G with different concentrations ranging from 1.0×10^{-5} mol/L to 1.0×10^{-9} mol/L. It can be seen that in a wide

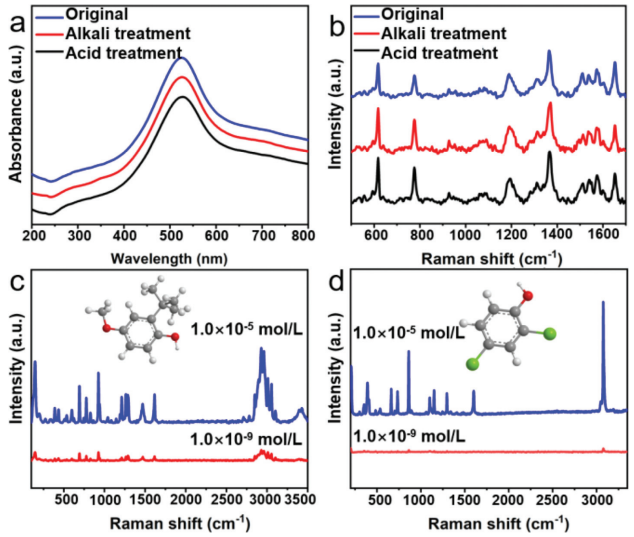

Fig. 3. Confirm the stability and universality of the ReO_3 microtubes substrate. (a) UV–vis-NIR absorption spectrum of ReO_3 microtubes substrate after acid etching and alkali etching. (b) The SERS spectrum of 1.0×10^{-6} mol/L R6G on the ReO_3 microtubes substrate after acid etching and alkali etching. (c) SERS spectrum of BHA and (d) SERS spectrum of 2,4-DCP.

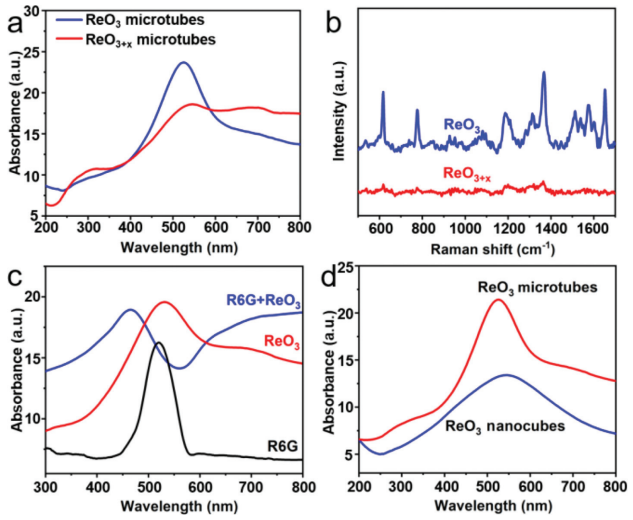

Fig. 4. Enhancement mechanism of ReO_3 microtubes. (a) UV–vis-NIR absorption spectra of ReO_3 microtubes and oxidized ReO_{3+x} microtubes. (b) SERS spectrum of 1.0×10^{-6} mol/L R6G on ReO_{3+x} microtubes substrate. (c) Absorption spectra for R6G on ReO_3 microtubes compared with pure ReO_3 microtubes and R6G. (d) UV–vis-NIR absorption spectrum of ReO_3 microtubes and ReO_3 nanocubes.

range of analyte concentration, these ReO_3 microtubes as SERS substrates can show excellent enhancement effects, and the lowest detection limit for R6G is 1.0×10^{-9} mol/L. This superior SERS sensitivity can be attributed to the electromagnetic field enhancement effect caused by the vigorous localized-SPR effect of these ReO_3 microtubules. In additon, we think that the good adsorption of ReO_3 microtubes also improves the detection sensitivity of this substrate material to a certain extent. Fig. S4 (Supporting information) shows the good adsorption capacity of ReO_3 microtubes.

Another criterion for measuring the practicality of SERS substrates is the signal repeatability of substrate testing. We use R6G at a concentration of 1.0×10^{-7} mol/L as the probe molecule to test the signal reproducibility of the ReO_3 microtube-substrate. As shown in Fig. 2c, the SERS spectra obtained from 50 randomly selected measurement points show that almost the same SERS spectrum intensity can be observed at different positions, suggesting the good uniformity of the ReO_3 microtube-substrate. Figs. S5 and S6 (Supporting information) show the two-dimensional Raman mapping images of the Raman signal of the ReO_3 microtube substrate itself and the SERS signal at the 612 cm^{-1} (R_1) characteristic peak of the 1.0×10^{-7} mol/L concentration of R6G on the ReO_3 substrate, respectively. Excellent preparation uniformity and test reproducibility are also demonstrated here. Furthermore, as shown in Fig. 2d, the signal relative standard deviation (RSD) of a total of 10,000 random points at 1362 cm^{-1} was calculated to convincingly demonstrate the high reproducibility of the prepared ReO_3 microtube substrate. The calculated results show that the signal RSD obtained from the substrate is only about 7.7%, which is significantly better than the commercial Au colloid substrates (~20%) [32].

In addition to the above two aspects, considering that in the Raman test, the substrate will be exposed to laser radiation with different powers, so the stability of the SERS substrate is also very important. Under normal circumstances, the chemical stability of transition metal oxides in the intermediate valence state is poor, such as $W_{18}O_{49}$ and Cu_2O with strong SERS activity. Fortunately, ReO_3 is one of the few very stable intermediate valence transition metal oxides similar to MoO_2 [33]. After immersing ReO_3 microtubes substrate in 2 mol/L NaOH solution and HCl solution for 5 h, the substrate can still exhibit an unabated SPR effect (Fig. 3a), and its SERS effect is not affected (Fig. 3b). XRD patterns, SEM images and HRTEM images also demonstrated their high chemical stability (Figs. S7-S10 in Supporting information).

In addition to R6G, the ReO_3 microtube SERS-substrate also has excellent detection sensitivity for some risk compounds of global interest. Butylated hydroxyanisole (BHA) is widely used in fried food because of its good anti-oxidation, anti-rancidity, good thermal stability and strong durability. However, the addition of BHA in food has certain safety hazards. Once excessive, it will cause certain toxicity to the human body, and even cause cancer risks. Therefore, it has been explicitly banned in the field of food addition in many countries. It can be seen from Fig. 3c that the ReO_3 microtube SERS-substrate has a good trace detection effect on BHA. 2,4-Dichlorophenol (hereinafter referred to as 2,4-DCP) is a recognized carcinogen and is a toxic environmental pollutant strictly controlled by the emission standards of various countries. On the ReO_3 microtube SERS substrate, even the concentration of 2,4-DCP was only 1.0×10^{-9} mol/L, it was sensitively detected (Fig. 3d). In addition, the controlled experiments also shown that the ReO_3 microtube-substrate also has a good detection capacity on rhodamine B (RhB) (Fig. S11 in Supporting information) and crystal violet (CV) (Fig. S12 in Supporting information), which displays a good detection universality.

Recent studies have shown that for semiconductor SERS substrates with high conductivity, the electromagnetic field enhancement caused by SPR effect and the chemical enhancement mechanism caused by interfacial charge transport play a role together, which is also applicable to the current ReO_3 substrate. Specifically, on the one hand, the strong localized-SPR effect makes ReO_3 microtubes have the physical enhancement mechanism dominated by electromagnetic hot spots similar to noble metals. In order to verify this point of view, we placed the sample in a muffle furnace and heated it in air for 0.5 h at 280 °C to obtain a taupe ReO_{3+x} (Fig. S13 in Supporting information). As the oxidation state increases, the free electron density decreases, the localized SPR peak of the sample drops sharply (Fig. 4a), and the corresponding SERS performance is also greatly reduced (Fig. 4b). However, it was found by SEM and XRD characterization that the microscopic morphology and crystal phase of the sample did not change (Figs. S14 and S15 in Supporting information), which suggests that only the change of valence state has occurred. These results above prove that the electromagnetic field enhancement caused by the

SPR effect does exist. On the other hand, when ReO_3 microtubes are immersed in R6G aqueous solution for 2 h, the UV–vis-NIR absorption spectra show that compared with the R6G aqueous solution and the unmodified ReO_3 microtubes, the absorption peak of the ReO_3 microtubes modified with R6G undergoes a clear blue shift (Fig. 4c). This phenomenon demonstrates that obvious interfacial charge transfer behavior occurs between ReO_3 microtube substrate and adsorbed R6G probe molecules. Based on the above results, it can be reasonably concluded that the ReO_3 substrate is affected by the double enhancement mechanism of SPR and chemical transmission.

In addition, to understand the effect of this microtubule structure assembled from nanocubes on the SERS effect, we further compared the localized-SPR effect and SERS effect of the dispersed nanocubes and the assembled microtubes. The nanocubes for comparison have similar morphology (Fig. S16 in Supporting information) and crystalline phase (Fig. S17 in Supporting information) as the cubes contained in the microtubes. Comparative studies have found that the localized-SPR effect of the ReO_3 microtubes is obviously stronger than that of the dispersed ReO_3 nanocubes (Fig. 4d). The reason may be that when the laser is irradiated on the ReO_3 microtube, part of the light passes through the nanotube wall and is reflected multiple times in the cavity, which increases the material's absorption of laser energy. However, this situation does not appear in the dispersed ReO_3 nanocubes, which directly causes the SPR effect of the ReO_3 microtubes to be much greater than that of the ReO_3 nanocubes.

In summary, a simple chemical method is developed to grow metallic ReO_3 self-assembled microtubes on the surface of silicon wafers. The rough surface and the grooved-cavity structure make the ReO_3 microtubes an efficient non-noble metal SERS substrate. Combined with their high Raman EF (8.9×10^5), sensitive detection limit (1.0×10^{-9} mol/L), high corrosion resistance, and low price, these ReO_3 microtubes have a good application prospect in the field of analytical chemistry.

Declaration of competing interest

The authors declare that they have no known competing financial interests or personal relationships that could have appeared to influence the work reported in this paper.

Acknowledgments

This work received financial support from the National Natural Science Foundation of China (No. 51771175) and the Science Foundation of State Administration of market supervision (No. 2021MK164).

Supplementary materials

Supplementary material associated with this article can be found, in the online version, at doi:10.1016/j.cclet.2022.05.086.

References

[1] C.L. Haynes, C.R. Yonzon, X. Zhang, R.P.V. Duyne, J. Raman Spectrosc. 36 (2005) 471–484.
[2] X. Qian, X.H. Peng, D.O. Ansari, Q. Yin-Goen, S. Nie, Nat. Biotechnol. 26 (2008) 83–90.
[3] J.H. Zhong, X. Jin, L. Meng, et al., Nat. Nanotechnol. 12 (2016) 132–136.
[4] C.Y. Li, J.C. Dong, X. Jin, et al., J. Am. Chem. Soc. 137 (2015) 7648–7651.
[5] S. Schlücker, Angew. Chem. Int. Ed. 53 (2014) 4756–4795.
[6] S. Van, T. Deckert-Gaudig, A. Mank, et al., Nat. Nanotechnol. 7 (2012) 583–586.
[7] C. Zhu, G. Meng, P. Zheng, et al., Adv. Mater. 28 (2016) 4871–4876.
[8] H. Liang, Z. Li, W. Wang, et al., Adv. Mater. 21 (2009) 4614–4618.
[9] X. Tan, L. Wang, C. Cheng, et al., Chem. Commun. 52 (2016) 2893–2896.
[10] S. Nie, S.R. Emory, Science 275 (1997) 1102–1106.
[11] K. Kneipp, Y. Wang, H. Kneipp, et al., Phys. Rev. Lett. 78 (1997) 1667–1670.
[12] J.F. Li, Y.F. Huang, Y. Ding, et al., Nature 464 (2010) 392–395.
[13] J.W. Jeong, M.M.P. Arnob, K.M. Baek, et al., Adv. Mater. 28 (2016) 8695–8704.
[14] D.K. Lim, K.S. Jeon, J.H. Hwang, et al., Nat. Nanotechnol. 6 (2011) 452–460.
[15] K.L. Wustholz, A.I. Henry, J.M. McMahon, et al., J. Am. Chem. Soc. 132 (2010) 10903–10910.
[16] Z. Liu, Z. Yang, B. Peng, et al., Adv. Mater. 26 (2014) 2431–2439.
[17] X. Zhang, Y. Zheng, X. Liu, et al., Adv. Mater. 27 (2015) 1090–1096.
[18] F. Gao, J. Lei, H. Ju, Anal. Chem. 85 (2013) 11788–11793.
[19] M. Fan, F.J. Lai, H.L. Chou, et al., Chem. Sci. 4 (2013) 509–515.
[20] S. Cong, Y.Y. Yuan, Z.G. Chen, et al., Nat. Commun. 6 (2015) 7800.
[21] X.C. Fan, M.Z. Li, Q. Hao, et al., Adv. Mater. Interfaces 6 (2019) 1901133.
[22] X.C. Fan, P.H. Wei, G.Q. Li, et al., ACS Appl. Mater. Interfaces 13 (2021) 51618–51627.
[23] L.L. Lan, X.Y. Hou, Y.M. Gao, et al., Nanotechnology 31 (2020) 055502.
[24] C. Liu, Q.C. Song, J.N. Chen, et al., Adv. Mater. Interfaces 6 (2019) 10.
[25] L. Tao, K. Chen, Z.F. Chen, et al., J. Am. Chem. Soc. 140 (2018) 8696–8704.
[26] J. Singh, S.Kumar Rishikesh, et al., J. Alloys Compd. 849 (2020) 11.
[27] A. Ferretti, D.B. Rogers, J.B. Goodenough, J. Phys. Chem. Solids 26 (1965) 2007–2011.
[28] C.N. King, H.C. Kirsch, T.H. Geballe, Solid State Commun. 9 (1971) 907–910.
[29] T. Tanaka, T. Akahane, E. Bannai, et al., J. Phys. C: Solid State Phys. 9 (1976) 1235–1241.
[30] K. Biswas, C.N.R. Rao, J. Phys. Chem. B 110 (2006) 842–845.
[31] S. Ghosh, H. Lu, S. Cho, et al., J. Am. Chem. Soc. 141 (2019) 16331–16343.
[32] H.Y. Chen, H.Lin M, C.Y. Wang, et al., J. Am. Chem. Soc. 137 (2015) 13698–13705.
[33] Q.Q. Zhang, X.S. Li, W.C. Yi, et al., Anal. Chem. 89 (2017) 11765–11771.